

# Glass Transition of Hard Sphere Systems: Molecular Dynamics and Density Functional Theory

Kang Kim and Toyonori Munakata

*Department of Applied Mathematics and Physics, Graduate School of Informatics,  
Kyoto University, Kyoto 606-8501, Japan*

(May 21, 2019)

The glass transition of a hard sphere system is investigated within the framework of the density functional theory (DFT). Molecular dynamics (MD) simulations are performed to study dynamical behavior of the system on the one hand and to provide the data to produce the density field for the DFT on the other hand. Energy landscape analysis based on the DFT shows that there appears a metastable (local) free energy minimum representing an amorphous state as the density is increased. This state turns out to become stable, compared with the uniform liquid, at some density, around which we also observe sharp slowing down of the  $\alpha$  relaxation.

PACS numbers: 64.70.Pf, 64.60.Cn, 61.20.Ja

Understanding of the universal mechanism of the glass transition is one of the major challenges in the current condensed matter physics. From a dynamical viewpoint, we would like to know how a drastic slowing down near the transition point (temperature or density) and an eventual exceeding of the relaxation time over the experimental time scale are realized [1,2]. Energetically or statically, it is asked whether a thermodynamic glassy state with the amorphous arrangement of particles has lower free energy than a liquid state of uniform density. In order to answer these questions, many efforts have been devoted to real experiments, computer simulations, and theories for the last decades.

As one of theories to study supercooled liquids and glasses, the density functional theory (DFT) is recently gathering much interests [3]. The DFT is now a conventional method to study the freezing [4,5] and other transitions. The glass transition has been investigated also based on the DFT by some workers [6–8]. Singh *et al.* produced the random close packing (RCP) of hard spheres based on the Bennett’s algorithm [9] and calculated the free energy from the DFT with the input density field supplied by the RCP data. They showed that the hard sphere glassy state becomes more stable than a uniform liquid at the critical density  $\sigma^3 n_g = 1.14$ , suggesting that there exists a kind of the thermodynamic (later called a random first order [7]) glass transition. Here  $\sigma$  is the hard sphere diameter and  $n_0$  is the number density of the system. It is remarked here that since the RCP configurations were produced by a kind of aggregation method, we can not study dynamical aspects of the glass transition found by the energetics based on DFT.

The purpose of this paper is first to produce a supercooled and a glassy state for a one-component hard sphere system, relying on the uniform compression molecular dynamics (MD) method recently developed by Lubachevsky and Stillinger [10] and then study both a dynamical and static properties of the states. Especially from the particle configuration data, we can discuss free

energy within the DFT framework. This MD approach, in conjunction with the DFT, enables us to study both dynamical and static aspects of the transition in contrast with the Bennett’s approach.

Our system consists of  $N = 1372$  identical hard spheres with the mass  $m$  and the diameter  $\sigma$  in a cubic box of volume  $V$  with periodic boundary conditions. Throughout this paper, the units of length and time are  $\sigma$  and  $\sqrt{\frac{m\sigma^2}{k_B T}}$ , respectively, where  $k_B$  is Boltzmann’s constant and  $T$  is the temperature. It should be noted that the temperature is fixed as  $k_B T = 1$  in the course of MD simulations and a non-dimensionalized quantity, say,  $\sigma^3 n_0$  ( $n_0 \equiv N/V$ ) is denoted by  $\tilde{n}_0$  hereafter.

To begin with, we briefly explain our MD method to obtain glassy states of a one-component hard sphere system. Employing the standard Alder and Wainwright algorithm [11,12], we first generate the equilibrium liquid state at the density  $\tilde{n}_0 = 0.86$ . It is well known that the fluid system freezes at  $\tilde{n}_0 \approx 0.94$ . To avoid the crystallization and obtain amorphous glassy states, Lubachevsky and Stillinger introduced a compressing (or quenching) procedure [10], in which they actually increased the diameter  $\sigma$  with a constant expanding rate during MD simulations. The dimensionless expanding rate  $\Gamma$  is defined as

$$\Gamma = \frac{d\sigma(t)}{dt} \sqrt{\frac{m}{k_B T}}, \quad (1)$$

and we took  $\Gamma = 0.01$  in our simulations. From the initial state  $\tilde{n}_0 = 0.86$ , we expanded each sphere with the rate  $\Gamma$  and could obtain various high density states, 0.86, 0.94, 1.02, 1.06, 1.10, 1.14, 1.18 and 1.21, without crystallization.

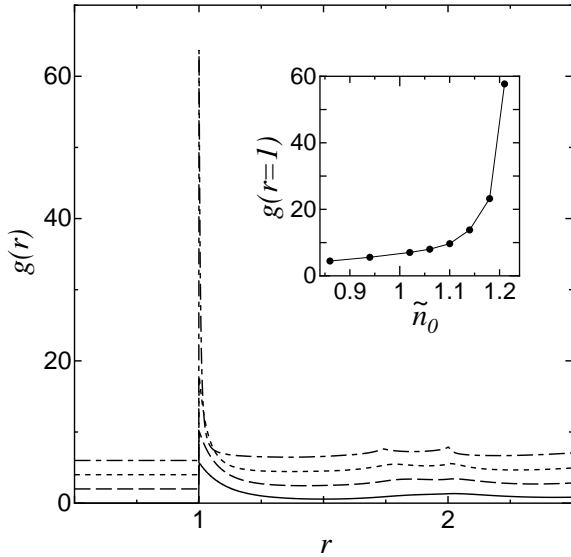


FIG. 1. The radial distribution function  $g(r)$  obtained for  $\tilde{n}_0 = 0.94$  (solid line), 1.06 (dashed line), 1.14 (short dashed line), and 1.21 (dot dashed line). Inset: contact value of radial distribution function  $g(r = 1)$  as a function of  $\tilde{n}_0$ .

We first study the static structure of the system. For the purpose the radial distribution function  $g(r)$ , which is defined by

$$g(r) = \frac{1}{n_0 N} \left\langle \sum_{i \neq j}^N \delta(\mathbf{r} + \mathbf{r}_i - \mathbf{r}_j) \right\rangle, \quad (2)$$

is calculated, where  $\mathbf{r}_i$  represents the positions of the  $i$ -th particle and  $\langle \dots \rangle$  denotes the ensemble average over different configurations. In Fig. 1, we plotted  $g(r)$  for the density  $\tilde{n}_0 = 0.94, 1.06, 1.14$ , and 1.21. We note that there is no sign of crystallization, which is reflected in sharp peaks of  $g(r)$  at some characteristic lattice spacings. Instead,  $g(r)$  for higher density shows the splitting of the second peak, which is a familiar characteristic of simple glassy liquids. Furthermore, we notice that the contact value  $g(r = 1)$  shows an anomalous increase as the density increases (see the inset), which corresponds to the fact that the pressure increases drastically with increasing  $n_0$ .

We next consider the dynamical aspects of the hard sphere glasses by calculating the incoherent intermediate scattering function  $F_s(q, t)$ , which is defined by

$$F_s(q, t) = \left\langle \frac{1}{N} \sum_{j=1}^N \exp[i\mathbf{q} \cdot \Delta \mathbf{r}_j(t; t_0)] \right\rangle_{t_0}, \quad (3)$$

where  $\Delta \mathbf{r}_j(t; t_0) = \mathbf{r}_j(t + t_0) - \mathbf{r}_j(t_0)$  is the displacement vector of the  $j$ -th particle in time  $t$ , and  $\langle \dots \rangle_{t_0}$  presents an average over initial times  $t_0$ . We note that the  $F_s(q, t)$  is one of the standard quantities in studies of dynamical properties of supercooled liquids and glasses [13,14]. In Fig. 2, we plotted the decay profiles of  $F_s(q, t)$  at a dimensionless wave number  $\tilde{q} \equiv q\sigma = 2\pi$  for  $\tilde{n}_0 = 0.94, 1.06, 1.14$ , and 1.21. We see in Fig. 2 that the function

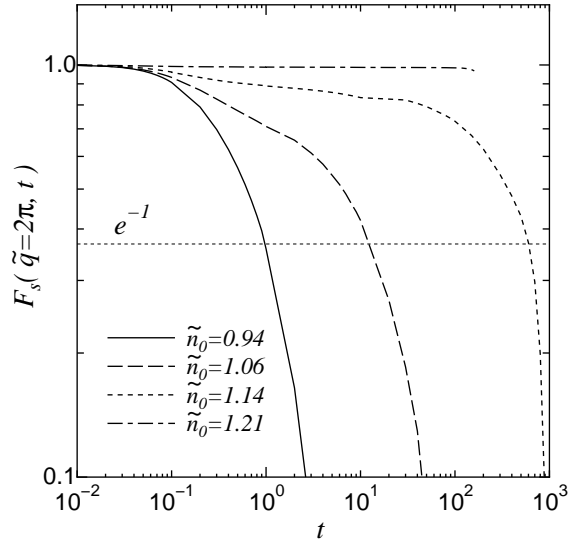


FIG. 2. Intermediate scattering function  $F_s(q, t)$  at a dimensionless wave number  $\tilde{q} = 2\pi$  for  $\tilde{n}_0 = 0.94$  (solid line), 1.06 (dashed line), 1.14 (short dashed line), and 1.21 (dot dashed line).

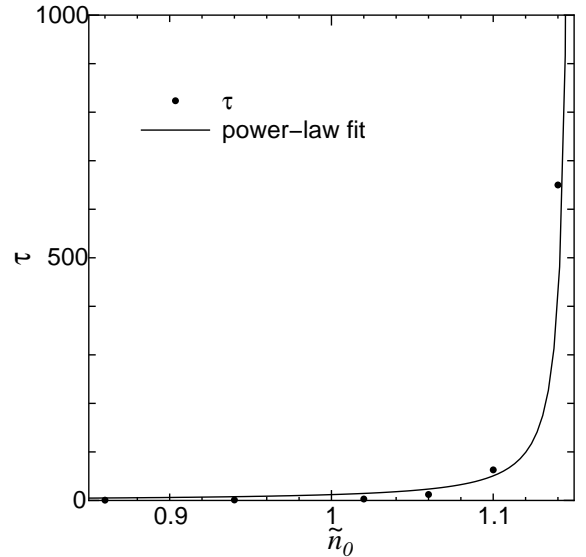


FIG. 3. Structural relaxation time  $\tau$  as a function of density  $n_0$  (closed circles). Solid line represents power-law fit  $(\tilde{n}_c - \tilde{n}_0)^{-\gamma}$  with  $\tilde{n}_c = 1.15$  and  $\gamma = 1.31$ .

$F_s(q, t)$  at  $\tilde{n}_0 = 0.94$  decays exponentially. Beyond the density  $\tilde{n}_0 = 1.06$ , however,  $F_s(q, t)$  exhibits the two-step (fast)  $\beta$ - and (slow)  $\alpha$ -relaxation, which is often mentioned as a characteristic sign of the slow relaxation in glass forming liquids. At the highest density  $\tilde{n}_0 = 1.21$ , the  $F_s(q, t)$  does not show any decaying behavior [15]. We here define the structural relaxation time  $\tau$  by  $F_s(\tilde{q} = 2\pi, \tau) = 1/e$  and plotted  $\tau$  as a function of  $\tilde{n}_0$  in Fig. 3. We notice in Fig. 3 that the relaxation time

$\tau$  shows a strong dependence on the density, which can be expressed by the power-law  $(\tilde{n}_c - \tilde{n}_0)^{-\gamma}$  with  $\tilde{n}_c \simeq 1.15$  and  $\gamma \simeq 1.31$  (solid line in Fig. 3).

We now consider energetics of the system based on the DFT and the configuration generated by the MD. Following Singh *et al.* [6], we employ the Ramakrishnan and Yussouff free energy functional [4]  $F[n]$ , which is given by

$$F[n] = F_{id} + F_{int}^{(2)} + F_{uni}, \quad (4)$$

where

$$F_{id} = k_B T \int n(\mathbf{r}) \ln \left[ \frac{n(\mathbf{r})}{n_0} \right] d\mathbf{r}, \quad (5)$$

$$F_{int}^{(2)} = -\frac{1}{2} k_B T \int \int [n(\mathbf{r}) - n_0] C(|\mathbf{r} - \mathbf{r}'|) \times [n(\mathbf{r}') - n_0] d\mathbf{r} d\mathbf{r}'. \quad (6)$$

Here,  $F_{id}$  and  $F_{uni}$  represent the ideal gas contribution and the excess free energy of the uniform liquid state  $n(\mathbf{r}) = n_0$ , respectively.  $F_{int}^{(2)}$  represents the second order term in the expansion around the uniform liquid state, thus all terms higher than second neglected. We note that  $C(\mathbf{r})$  is the direct correlation function of the uniform liquid with the density  $n_0$  [16].

In order to evaluate the free energy of the system, we need the trial density field  $n(\mathbf{r})$ , for which we employ a conventional Gaussian superposition. That is, the density field  $n(\mathbf{r})$  is expressed by a sum of Gaussians with the centers located at  $N$  sites  $\{\mathbf{r}_i\}$ , which are given by our MD simulation.

$$n(\mathbf{r}) = \sum_{i=1}^N \left( \frac{\alpha}{\pi} \right)^{3/2} \exp[-\alpha(\mathbf{r} - \mathbf{r}_i)^2] \equiv \sum_{i=1}^N z(\mathbf{r}; \mathbf{r}_i), \quad (7)$$

where  $\alpha^{-1}$ , a variational parameter for the calculation of the free energy, corresponds to the inverse of the mean square displacement of each particle. Small (large)  $\alpha$  represents the uniform liquid (localized amorphous) state.

When  $\alpha$  is very large,  $F_{id}$  is asymptotically represented by [6]

$$F_{id}(\alpha) \sim N k_B T \left[ \left\{ \frac{3}{2} \ln \left( \frac{\alpha}{\pi} \right) - \frac{3}{2} \right\} - \ln n_0 \right]. \quad (8)$$

For a small  $\alpha$  region, we calculated the integral Eq. (5) numerically. We confirmed that  $F_{id}$  approaches 0 when  $\alpha \rightarrow 0$  and noticed that  $F_{id}$  begins to coincide with the value of Eq. (8) for  $\alpha \simeq 20$ .

It is easy to see that the interaction term  $F_{int}$  can be divided into three parts as [6]

$$F_{int}^{(2)}(\alpha) = -\frac{1}{2} N k_B T \left\{ F_{int,1}(\alpha) + F_{int,2}(\alpha) - n_0 \int C(r) dr \right\}, \quad (9)$$

where  $F_{int,1}(\alpha)$  represents the self-interaction of a single Gaussian,

$$F_{int,1}(\alpha) = \int \int z(\mathbf{r}; \mathbf{0}) C(|\mathbf{r} - \mathbf{r}'|) z(\mathbf{r}'; \mathbf{0}) d\mathbf{r} d\mathbf{r}', \quad (10)$$

and  $F_{int,2}(\alpha)$  represents the interaction between the two distinct Gaussians,

$$F_{int,2}(\alpha) = n_0 \int g(r_1) d\mathbf{r}_1 \int \int z(\mathbf{r}; \mathbf{0}) C(|\mathbf{r} - \mathbf{r}'|) \times z(\mathbf{r}'; \mathbf{r}_1) d\mathbf{r} d\mathbf{r}'. \quad (11)$$

The pair distribution function  $g(r)$  in this equation is determined from the MD simulation. When the density becomes very large, it is rather difficult to obtain reliable numerical values of  $C(r)$  from the (computer) experimental  $g(r)$ . This is because  $g(r)$  becomes sharper and sharper for a compressed system (see Fig.1) and its Fourier transform, which is necessary in dealing with the Ornstein-Zernike relation [16], becomes more and more unreliable. Under this condition, we use the Henderson-Grundke expression for  $C(r)$ , which is known to be reliable, though empirical, even for high density hard sphere liquid [17].

We calculate total free energy per particle relative to uniform state:

$$\Delta f(\alpha) = \frac{F_{id}(\alpha) + F_{int}^{(2)}(\alpha)}{N k_B T}, \quad (12)$$

as a function of the localization parameter  $\alpha$ , and look for a free energy minimum for various density states. In Fig. 4, we show  $\Delta f(\alpha)$  for  $\tilde{n}_0 = 0.94, 1.06, 1.14,$  and  $1.21$ . It is seen in Fig. 4 that the free energy local minimum at finite  $\alpha$  appears for the density  $\tilde{n}_0 \gtrsim 1.06$ . As is mentioned in Ref. [6], the local minimum appears as the

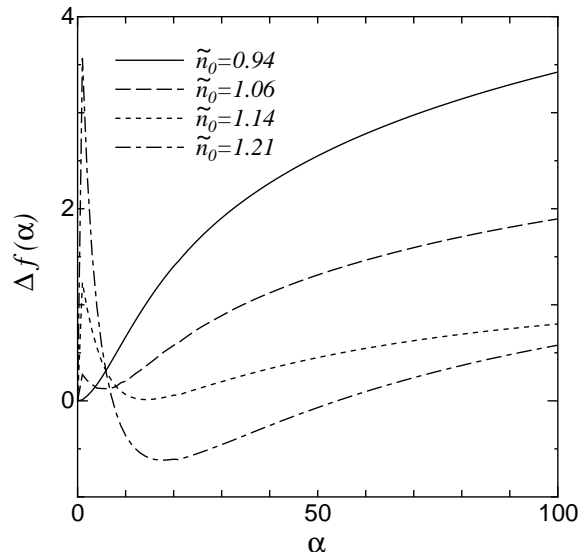


FIG. 4. Total free energy per particle relative to uniform liquid  $\Delta f(\alpha)$  as a function of localization parameter  $\alpha$  for  $\tilde{n}_0 = 0.94$  (solid line),  $1.06$  (dashed line),  $1.14$  (short dashed line), and  $1.21$  (dot dashed line).

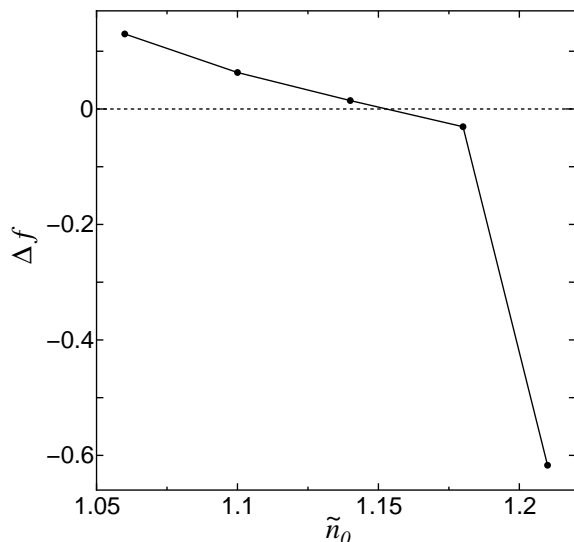


FIG. 5. Free energy difference between the local minimum and uniform liquid  $\Delta f$  as a function of density  $\tilde{n}_0$ .

result of the competition between the ideal gas (simple increasing function of  $\alpha$ ) and the interaction terms. In Fig. 5, we plotted the free energy at the local minimum  $\Delta f$  as a function of the density  $n_0$ . From Fig. 5, we find that the free energy difference between the uniform and localized states crosses  $\Delta f = 0$  line at  $\tilde{n}_0 \simeq 1.15$ , which corresponds to the liquid-glass transition density  $n_g$  from the energetics based on the DFT. In passing we note that our (first order) glass transition density  $\tilde{n}_g \simeq 1.15$  is rather close to the one  $\tilde{n}_g \simeq 1.14$  found in Ref. [6].

Finally, we compare our results on energetics with dynamical informations supplied by our MD. We find in Fig. 2 that the intermediate scattering function  $F_s(q, t)$  begins to exhibit the two-step  $\beta$ - and  $\alpha$ - relaxation at the density  $\tilde{n}_0 \simeq 1.06$ , which corresponds precisely to the density where the free energy local minimum begins to appear in our DFT (see Fig. 4). Turning to the relaxation time  $\tau$ , we recall that the density dependence of  $\tau$  can be described by the power-law form  $(\tilde{n}_c - \tilde{n}_0)^{-\gamma}$  with  $\tilde{n}_c \simeq 1.15$ . This density seems to correspond to the density beyond which the localized glassy state is more stable than the uniform liquid in the present DFT. From these results, we consider that the DFT based energetics and dynamical behaviors related to slow dynamics are well correlated with each other.

In this paper, we reconsidered DFT approach to the glass transition in the hard sphere system, which was first undertaken by Singh *et al.* We obtained hard sphere glasses by MD simulations without recourse to the Bennett's algorithm and the information on particle configurations produced by the MD simulations are used as input data when the free energy is calculated based on

the DFT. While only the uniform liquid state is stable at low density, the free energy local minimum appears at high density  $\tilde{n}_0 \gtrsim 1.06$ . This metastable glassy state becomes stable relative to uniform liquid at  $\tilde{n}_0 \simeq 1.15$ . Slow relaxation as represented by the time correlation function turned out to be consistent with the energetics based on the DFT.

One of the authors (K. K.) would like to thank Dr. R. Yamamoto for helpful discussions and suggestions. He also thanks Associate Professor A. Yoshimori and Dr. H. Frusawa for useful discussions. He is benefited from many discussions with lecturers and participants at the Les Houches Summer School 2002.

- 
- [1] J. Jäckle, Rep. Prog. Phys. **49**, 171 (1986).
  - [2] M. D. Ediger, C. A. Angell, and S. R. Nagel, J. Phys. Chem. **100**, 13200 (1996).
  - [3] For reviews, see A. D. J. Haymet, Ann. Rev. Phys. Chem. **38**, 89 (1987); D. W. Oxtoby, in *Liquid, Freezing, and the Glass Transition*, edited by J. P. Hansen, D. Levesque, and J. Zinn-Justin (Elsevier, New York, 1990).
  - [4] T. V. Ramakrishnan and M. Yussouff, Phys. Rev. B **19**, 2775 (1979).
  - [5] A. D. Haymet and D. W. Oxtoby, J. Chem. Phys. **74**, 2559 (1981); D. W. Oxtoby and A. D. Haymet, *ibid.* **76**, 6262 (1982).
  - [6] Y. Singh, J. P. Stoessel, and P. G. Wolynes, Phys. Rev. Lett. **54**, 1059 (1985).
  - [7] X. Xia and P. G. Wolynes, Proc. Natl. Acad. Sci. **97**, 2990 (2000).
  - [8] C. Kaur and S. P. Das, Phys. Rev. Lett. **86**, 2062 (2001).
  - [9] C. H. Bennett, J. Appl. Phys. **45**, 2727 (1972).
  - [10] B. D. Lubachevsky and F. H. Stillinger, J. Stat. Phys. **60**, 561 (1990); B. D. Lubachevsky, F. H. Stillinger, and N. Pinson, *ibid.* **60**, 501 (1991).
  - [11] B. J. Alder and T. E. Wainwright, J. Chem. Phys. **31**, 459 (1959)
  - [12] M. P. Allen and D. J. Tildesley, *Computer Simulations of Liquids* (Clarendon Press, Oxford, 1987).
  - [13] W. Kob and H. C. Andersen, Phys. Rev. E **52**, 4134(1995).
  - [14] R. Yamamoto and A. Onuki, Phys. Rev. E **58**, 3515(1998).
  - [15] It is remarked here that due to frequent collisions under compressed situation a long time simulation at high density is prohibitively difficult to perform.
  - [16] J. P. Hansen and I. R. McDonald, *Theory of Simple Liquids* (Academic Press, London, 1986).
  - [17] D. Henderson and E. W. Grundke, J. Chem. Phys. **63**, 601 (1975).